

Collective dynamics of trail-interacting particles

Paul Pineau,^{*} Samuel Bell, and Raphaël Voituriez[†]
Laboratoire Jean Perrin, CNRS/Sorbonne Université, Paris, France

Ram M. Adar[‡]

Department of Physics, Technion – Israel Institute of Technology, Haifa 32000, Israel

Trail interactions occur when past particle trajectories bias future motion, rendering the system out of thermodynamic equilibrium. While such systems are abundant in nature, their understanding is limited to the single-particle level or phenomenological mean-field theories. Here, we introduce a minimal model of many trail-interacting particles that extends this paradigm to the fluctuating collective level. Particles diffuse while depositing long-lasting repelling/attracting trails that act as a shared memory field, coupling their dynamics across time and space. Using stochastic density functional theory, we derive fluctuating hydrodynamic equations and analyze analytically and numerically the resulting behaviors. We show that memory, coupled with fluctuations, fundamentally reshapes collective dynamics; In the repulsive case, the particle density displays superdiffusive spreading characterized by transient clustering and ballistic motion; In the attractive case, the system condensates in finite time into frozen, localized states. Our results establish general principles for trail-interacting systems and reveal how persistent fields generate novel instabilities and self-organization.

Many living and synthetic agents modify their environment by depositing persistent trails that bias their subsequent motion. Examples include ants laying pheromone traces [1, 2], cells navigating via self-secreted cues [3–5], and self-propelled droplets guided by trails of micelles [6, 7]. In all cases, trails introduce a shared memory of past motion that renders these systems out of equilibrium, and drives long-ranged spatial and temporal correlations. Despite the ubiquity of trail-interacting systems, their collective behavior remains poorly understood.

Theoretical studies of memory-driven motion have mostly focused on self-interacting random walks, where a single particle’s trajectory is influenced by its own past [8–12]. Such non-Markovian dynamics result in rich phenomena, including localization, anomalous diffusion, and aging. By contrast, far less is known about the collective behavior of particles coupled through the trails they all generate. As the dynamics depends on the full system’s history, the collective description cannot be reduced to instantaneous pairwise interactions. Existing approaches rely mainly on mean-field or hydrodynamic descriptions [13–17], as well as numerical simulations [16–21].

In this Letter, we introduce and analyze a minimal model of trail-interacting particles that extends single-particle self-interacting walks to the fluctuating hydrodynamic level. The model couples the motion of diffusing particles to a non-decaying memory field that records their trajectories and biases subsequent motion. Using stochastic density functional theory and large-scale simulations, we show how environment-stored memory reshapes collective dynamics, leading to nontrivial scaling regimes, propagating modes, and condensation phenomena. Our framework establishes general principles for the study of systems with long-lived self-generated fields and opens new directions for exploring memory-driven self-

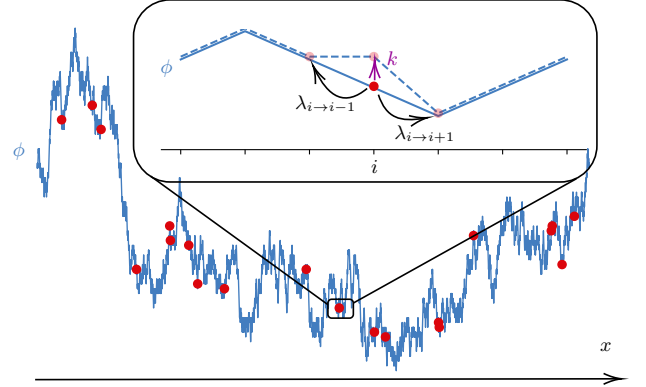


FIG. 1: Schematic illustration of the model. Each particle (in red) lives in a potential landscape ϕ (in blue). Inset: two possible dynamics of a single particle: hopping to neighboring sites with rates $\lambda_{i\pm 1}$ and trail deposition with rate k . One deposition increase locally ϕ by 1 (purple event). Translucent red dots represents the three possible future state of the particle.

organization in statistical physics.

Model. We formulate a lattice model of trail-interacting particles, sketched in Fig. 1. For simplicity, we focus on the one-dimensional case. We consider N particles distributed along L/a lattice sites, where L is the system size and a the lattice constant. The state of each site i is described by its particle occupancy ρ_i and trail content ϕ_i . The coupled dynamics of both fields, defined for convenience in continuous time t , is driven by two types of independent transition events: (i) hopping of a particle from site i to a neighboring site $i \pm 1$, with rate $\rho_i \lambda_{i \rightarrow i \pm 1} = 2\rho_i k_{tr} / (1 + \exp[H(\phi_{i \pm 1}) - H(\phi_i)])$ and (ii) deposition of a trail unit, with rate $\rho_i k$. Here, k_{tr} is a typical single particle translation rate, related to the diffusion constant D according to $D = k_{tr} a^2$, and $H(\phi_i)$

acts as a Hamiltonian that biases the hopping rate according to differences in trail concentration in neighboring sites. Finally, k is a typical trail deposition rate per particle. Note that the trail is not degraded in this model, and most importantly does not diffuse, in contrast to the broad class of models of autochemotactic biological systems [22–25] or autophoretic particles [19, 26, 27]. It thus acts as a persistent memory field for particle trajectories. The model can be generalized to additional trail dynamics (such as degradation or deterministic deposition) and higher spatial dimensions in a straightforward manner.

The lattice dynamics can be mapped to a stochastic density functional theory (SDFT) in the continuum limit, using exact path-integral methods [28–31]. The resulting equations are [32]

$$\begin{aligned}\partial_t \rho &= D \partial_{xx} \rho + D \partial_x [\rho \partial_x H(\phi)] + \partial_x \left(\sqrt{2D\rho} \eta \right), \\ \partial_t \phi &= k\rho + \sqrt{k\rho} \xi,\end{aligned}\quad (1)$$

and constitute the central result of this paper. The stochastic nature of the dynamics is manifested in noise terms in the particle and trail dynamics, η and ξ , respectively. They are both Gaussian white noises with $\langle y \rangle = 0$ and $\langle y(t, x) y(t', x') \rangle = \delta(t - t') \delta(x - x')$, where $y = \eta, \xi$, while $\langle \xi \eta \rangle = 0$. Importantly, the mapping between the lattice dynamics and Eq. (1) is exact in the $a \rightarrow 0$ limit, except for the ξ term that approximates the true shot noise of the Poissonian deposition process. This approximation however becomes exact at long times.

Despite the apparent complexity and intrinsic non-Markovian nature of trail-mediated interactions, which lie beyond the classical framework of pairwise interactions, Eq. (1) shows that the particle density obeys an equation of the Dean-Kawasaki form [33, 34] with transparent physical interpretation. It expresses the conservation of particles undergoing diffusion and advection according to the effective Hamiltonian $H(\phi)$, with multiplicative noise encoding particle number fluctuations. This apparent simplicity – with no explicit interaction term – comes at the cost of a coupling to the additional trail density field ϕ , which undergoes a simple irreversible first-order growth kinetics with source term ρ and multiplicative noise originating from the stochastic deposition. We focus below on the example $H = h\phi$ for simplicity. We analyze the linear stability of the system within mean field (MF) and proceed by analyzing correlations beyond MF in both the repulsive and attractive cases ($h > 0$ and $h < 0$, respectively).

Linear stability analysis and time dependent structure factors. We consider first a simple uniform state with $\rho(t = 0, x) = \rho_0$ and $\phi(t = 0, x) = \phi_0$. Without loss of generality, we set $\phi_0 = 0$. We linearize the equations around the uniform dynamics by introducing the first-order corrections in the fields $\delta\rho(t, x) = \text{Re}[\delta\rho(t, q) \exp(iqx)]$ and similarly for ϕ , so that $\rho = \rho_0 + \delta\rho$ and $\phi = k\rho_0 t + \delta\phi$. Furthermore, we make use of

dimensionless forms, where lengths are normalized by the system size L , times by $\tau = L^2/D$, and densities by the average density ρ_0 . For simplicity, we use the same notations, such that $\rho \rightarrow \rho_0 \rho$, $\phi \rightarrow \rho_0 \phi$, $\partial_t \rightarrow \partial_t/\tau$, $q \rightarrow q/L$, $k \rightarrow k/\tau$, and $h \rightarrow h/\rho_0$. This leads to

$$\partial_t \delta\rho + q^2 \partial_t \delta\rho + khq^2 \delta\rho = \frac{\Xi}{\sqrt{N}}, \quad (2)$$

with the noise term $\Xi = \sqrt{2}iq\partial_t \eta - \sqrt{k}hq^2 \xi$ and $N = \rho_0 L$ the total number of particles. This is the equation of a damped harmonic oscillator, where q^2 is the friction coefficient, originating in diffusion, while khq^2 plays the role of the spring constant, originating in the memory field. It is clear that the system is linearly unstable for all q for an attractive interaction ($h < 0$), corresponding to a negative spring constant. Explicitly, the dispersion relation is given by $i\omega = -q^2/2 \pm \sqrt{(q^2/2)^2 - khq^2}$.

To go beyond the linear stability analysis, we make use of our exact determination of the noise amplitudes and predict the dynamics of the static structure factors of the dimensionless particles density $S_\rho(t, q) = \langle \delta\rho(t, -q) \delta\rho(t, q) \rangle$ and dimensionless trail density $S_\phi(t, q) = \langle \delta\phi(t, q) \delta\phi(t, -q) \rangle$. Eq. (2) is solved and averaged over noise realizations, leading to [32]

$$\begin{aligned}S_\rho(t, q) &= \frac{q^2}{N} \int_0^t ds [2G'^2(s, q) + kh^2 q^2 G^2(s, q)], \\ S_\phi(t, q) &= \frac{k}{N} \int_0^t ds [(G'(s, q) + q^2 G(s, q))^2 + 2khq^2 G^2(s, q)],\end{aligned}\quad (3)$$

where the kernel is defined as

$$G(\tau, q) = \frac{e^{-q^2 \tau/2}}{\sqrt{(q^2/2)^2 - q^2 kh}} \sinh \left(\tau \sqrt{(q^2/2)^2 - q^2 kh} \right), \quad (4)$$

and $G' = \partial G / \partial \tau$. These results rely on the linearized dynamics and are valid for sufficiently small noise amplitudes. The explicit time dependence that we find captures the transient dynamics from the uniform initial condition, which is a stationary state of the MF dynamics of the particle density field, but not of the full fluctuating dynamics in both the repulsive and attractive cases. In what follows, we analyze the results of Eqs. (3)-(4), while comparing between the analytical predictions and lattice simulation results (see SM [32] for details). We consider the repulsive (linearly stable) and attractive (linearly unstable) cases separately, as they display qualitatively different behaviors.

Repulsive case ($h > 0$). In the repulsive case, the uniform state is linearly stable as shown above. Nevertheless, both particles and trail structure factors display a non-trivial steady state and transient dynamics, which are captured remarkably well, with no adjustable parameter, by our linear analysis (see Fig. 2a,b). At long times

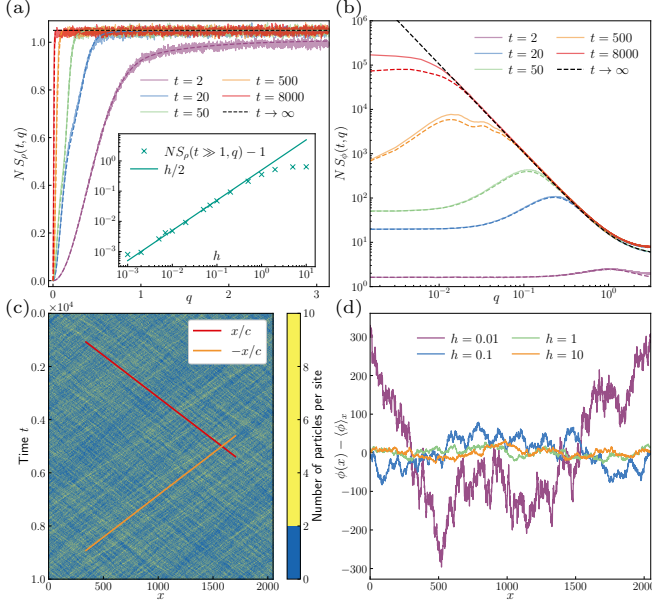


FIG. 2: (Color online) Results in the repulsive case ($h > 0$). (a+b) Density- and trail structure factors as a function of the wavevector at different times. Simulation results are plotted as solid lines and the theoretical prediction of Eq. (3) as dashed lines. The asymptotic value for long times is plotted in dashed black. Inset of (a) shows how the long-time density structure factor scales with h , according to the simulations (symbols) and theory (solid line). (c) Kymograph of density as a function of space and time. The texture indicates that low- and high-density fluctuations travel at a velocity $\pm c = \pm \sqrt{hk}$. (d) Characteristic trail profiles at long times for different h values, according to the simulations.

and for a non vanishing $h > 0$, the trail structure factor is found to reach a steady state (see Fig.2b,d)

$$S_\phi(t, q) \underset{t \rightarrow \infty}{\approx} \frac{k(2+h) + q^2}{2hNq^2}. \quad (5)$$

This result interpolates between two simple limits: for small wavevectors, $q \ll \sqrt{k(2+h)}$, the structure factor scales as $\sim 1/q^2$, which is consistent with a trail profile $\phi(x)$ that behaves as a Brownian path of effective diffusion coefficient $k(2+h)/(4h)$ in quantitative agreement with simulations (see Fig.2b). Note that such steady state profile is consistent with both Edwards-Wilkinson and Kardar-Parisi-Zhang models [35, 36]. Interestingly, the trail field was found earlier to be exactly Brownian in the case of a single true self-avoiding walker in infinite space with comparable trail mediated dynamics [8]. A non-linear analysis, necessary to fully characterize the trail field, is left for further work. For large wavevectors, $q \gg \sqrt{k(2+h)}$, the structure factor scales as $\sim q^0$, due to the noise in the deposition process itself, which induces Poissonian fluctuations. Of note, the $h \rightarrow 0$ limit is singular in Eq.(5) and indicates that a non-vanishing interaction with the trail field is necessary for the trail fluctuations to reach a steady state. The case $h = 0$ is discussed in SM [32].

For $h > 0$, the particle static structure factor also

reaches a steady state, which is found analytically (and verified numerically in Fig. 2a) to be independent of q :

$$N S_\rho(t, q) \underset{t \rightarrow \infty}{\approx} 1 + h/2. \quad (6)$$

This indicates that, despite their apparent complexity, trail-mediated interactions lead at steady state only to effectively zero-range attractive interactions among particles: the static structure factor is that of (on average) $N/(1 + h/2)$ independent one-lattice-site clusters of $1 + h/2$ particles. In particular, despite repulsive interactions with the trail field, there is no sign of effective repulsion among particles at steady state.

To decipher the microscopic origin of such zero range attractive interactions, we analyse the dynamic structure factor $S_\rho(\omega, q) = \langle |\delta\rho(\omega, q)|^2 \rangle$, which can be obtained at steady state upon Fourier transformation in time domain of Eq.2. This yields (see [32])

$$S_\rho(\omega, q) = \frac{1}{Nq^2} \frac{2 + \frac{hc^2q^2}{\omega^2}}{1 + \frac{\omega^2}{q^4} \left(1 - \frac{c^2q^2}{\omega^2}\right)^2} \equiv \frac{1}{Nq^2} g\left(\frac{\omega}{q^2}, \frac{\omega}{cq}\right) \quad (7)$$

where $c = \sqrt{hk}$ is a typical velocity and $g(u, v)$ the scaling function. The dynamic structure factor of the trail field is obtained along the same method and given in [32], where the quantitative agreement with numerical simulations is shown. For $q \gg c$, the structure factor is found to satisfy a single diffusive scaling $S_\rho(\omega, q) \sim g(\omega/q^2, v \rightarrow \infty)/q^2$, identical to that of non interacting diffusing particles, indicating that trail-mediated interactions are irrelevant at short length scales. In turn, for $q \ll c$ we find a ballistic scaling $S_\rho(\omega, q) \sim g(u \rightarrow \infty, \omega/(cq))/q^2$ with a pole for ω, q satisfying the dispersion relation $\omega = \pm cq$. This reveals the emergence of traveling waves of velocity c induced by trail-mediated interactions at large length scales, which are indeed observed in numerical simulations with quantitative agreement (see Fig.2c).

Such traveling waves share similarities with wave patterns observed for repulsive autophoretic particles [19] and solutions of the Fisher-KPP equation [37]. It can also be understood in terms of a non-reciprocal interaction, where the trail field is “attracted” to the particles who, in turn, are repelled by the trail. Furthermore, these waves provide a microscopic mechanism to account for the effective zero-range attractive interaction observed above: particles in the same wave packet experience the same local trail profile and form transient clusters. We note that the MF version of Eq. (1) further allows for traveling-front solutions, whose profile can be found analytically from the nonlinear equations [32]. They require non-periodic boundary conditions.

To validate the applicability of our hydrodynamic equations Eq. (1) beyond linear order, we now analyze within MF the spreading dynamics of a localized initial condition, $\rho(0, x) = N\delta(x)$ and $\phi(0, x) = 0$, keeping $h > 0$. We look for self-similar solutions of the form

$\rho(t, x) = t^{-\alpha} f(x/t^\alpha)$, $\phi(t, x) = t^{-\alpha+1} F(x/t^\alpha)$ in the limit $x, t \rightarrow \infty$ with $u = x/t^\alpha$ finite. Substituting in Eq. (1), while setting $\eta, \xi = 0$ yields

$$\begin{aligned} -\alpha t^{-\alpha-1} (fu)' &= t^{-3\alpha} f'' - h t^{1-4\alpha} (fF')' \\ kf &= -\alpha u F' + (1 - \alpha) F. \end{aligned} \quad (8)$$

The analysis of this equation shows that two distinct scaling regimes emerge, and allows for an exact determination of α . At early times ($t \ll 1/(hk)^2$), the trail field remains small, particle diffusion controls the dynamics and, as expected, $\alpha = 1/2$. After a transient regime ($t \gg 1/(hk)^3$), the long time dynamics controlled by trail-mediated advection sets in, leading to a superdiffusive scaling $\alpha = 2/3$ [32]. In this regime, the coupled non-linear equations for $f(u)$ and $F(u)$ can be solved analytically (see [32]) and yield

$$\begin{aligned} \rho(t, x) &= \frac{1}{t^{2/3}} \frac{1}{3kh} \left[\frac{y_0^2}{3} + \frac{x^2}{t^{4/3}} \right] \Theta \left(y_0^2 - \frac{x^2}{t^{4/3}} \right) \\ \phi(t, x) &= t^{1/3} \frac{1}{3h} \left[y_0^2 - \frac{x^2}{t^{4/3}} \right] \Theta \left(y_0^2 - \frac{x^2}{t^{4/3}} \right) \end{aligned} \quad (9)$$

where Θ is the Heaviside function and $y_0 = (9Nkh/4)^{1/3}$ follows from the particle number conservation and positiveness of ϕ . This describes a superdiffusively expanding front of width $\sim t^{2/3}$, with a trail field growing as $t^{1/3}$ in amplitude. As shown in Fig. 3, these expressions quantitatively reproduce the numerical data without adjustable parameters for small h values. Of note, the same scaling exponent $\alpha = 2/3$ was found for a single true self-avoiding random walk with similar trail-mediated dynamics [8, 38] and for a single autophoretic particle [27] with, however, a strikingly distinct scaling function for the particle probability density [39, 40]. This highlights the importance of trail mediated interactions in the spreading dynamics. A similar analysis of the superdiffusive regime has been performed independently in [17], based on MF hydrodynamic equations derived in [13] that however do not cover all time regimes.

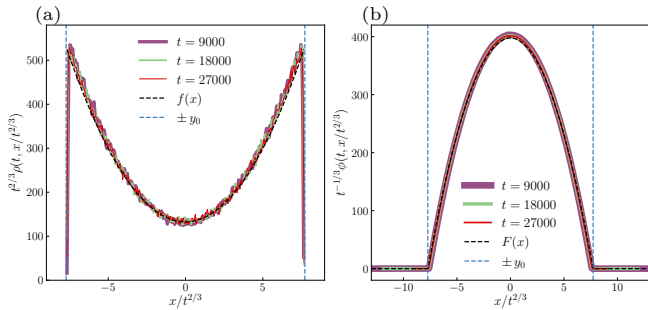


FIG. 3: Rescaled profiles of (a) the particle density and (b) the trail density, compared with the theoretical predictions of Eq. (9). Simulations correspond to $N = 4096$, $h = 0.05$, $k = 1$, averaged over 50 realizations. The collapse confirms the superdiffusive scaling $\alpha = 2/3$ and the compact support predicted analytically.

Attractive case ($h < 0$). The attractive case is linearly unstable, as shown above. Therefore, the analytical results obtained by analyzing perturbations around the uniform steady state are expected to hold only at short times. This is verified quantitatively by our simulation results in Fig. 4a. At longer times, we find numerically that particles condensate in well-separated sites and remain frozen (Fig. 4c,d), generalizing earlier results showing the self trapping of single particles [41]. Qualitatively, once a condensate starts to form, the trail field at that site builds up, creating an increasingly deep potential well from which the particles cannot escape.

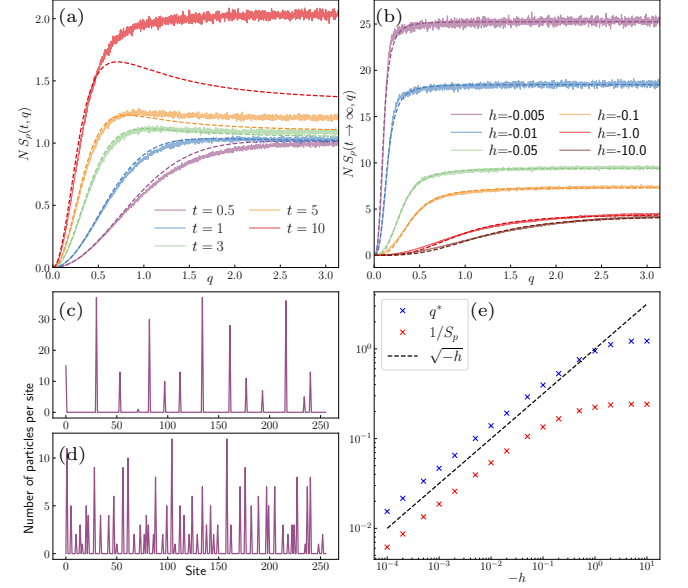


FIG. 4: (Color online) Results in the attractive case ($h < 0$). (a+b) Density structure factor as a function of the wavevector at different times (a) and different h values at long times (b). Simulation results are plotted as solid lines, theoretical prediction of Eq. (3) as dashed lines for (a), and sigmoid-type fit as dashed lines for (b). (c+d) Snapshots of the density profile in permanent state for $h = 0.05, k = 0.1$ (c) and $h = 0.1, k = 1$ (d). (e) The characteristic wavevector q_* and asymptotic value of the structure factor S_p as a function of h for $k = 1$. The theoretical scaling is plotted in dashed black.

While the system is far from the initial uniform steady state, the density structure factor can be well approximated by the following ansatz, which is suggested by the short time linear dynamics. The steady state can be understood in terms of a single parameter - the characteristic wavevector q_* that corresponds to a separation of $2\pi/q_*$ between condensates. For $q > q_*$, the structure factor is dominated by the overlap between particles in each condensed site. We denote the asymptotic plateau value $S_\rho(t \gg 1, q \gg 1) = S_p$ and estimate $S_p = (2\pi/q_*)^{-1} (N \times 2\pi/q_*)^2 = N^2 2\pi/q_*$, where the first term estimates the number of condensates and the second one - the number of particles in each condensate squared. This results is validated by our simulations

(Fig. 4e). We consider a sigmoid-type transition between small and large q values, following $S_\rho = S_p q^n / (q^n + q_*^n)$, where $n = 3$ is our ad-hoc choice to fit to the simulation results (Fig. 4b). The steady state in the attractive case is thus fully characterized by q_* .

The scaling of q_* with h can be deduced by comparing the timescales of diffusion at the scale $1/q_*$, and of growth of the trail-mediated interaction $h\phi$ to significantly impact transport. For weak interactions, equating the rates q_*^2 for diffusion and $k|h|$ for the growth of the trail-mediated interaction, we find $q_* \sim \sqrt{k|h|}$, as validated by simulations (Fig. 4e). Note that $|h| \ll 1$ corresponds to a single condensate, similar to a zero-range process [42]. For strong interactions, however, a single deposition is enough to induce condensation. We thus estimate the rate of a single deposition by any of the particles found along a distance $\sim 1/q_*$. This rate scales as k/q_* and, equating to the diffusion rate, we find $q_* \sim k^{1/3}$, as validated by simulations [32].

Discussion. We have introduced a minimal model for trail-interacting particles that extends the physics of self-interacting random walks from single-particle to collective dynamics and goes beyond available mean-field hydrodynamic descriptions. By combining stochastic density functional theory and simulations, we demonstrated how the coupling to the persistent trail field that encodes the memory of the system fundamentally alters transport and fluctuations, leading to ballistic clustering, propagating modes, and condensation. These results highlight trail mediated memory as a generic mechanism for self-organization, distinct from direct interactions or external fields. Beyond providing a unifying framework for trail-mediated processes in biological and synthetic systems, our study suggests new directions for exploring memory-driven phenomena in nonequilibrium statistical physics, from collective migration and chemotaxis to artificial active materials.

Acknowledgements. We thank J. Brémont, O. Bénichou, and Y. Kafri for useful discussions. Support from ERC synergy grant SHAPINCELLFATE and Israel Science Foundation (ISF) under Grant No. 444/25 is acknowledged.

* paul.pineau@sorbonne-universite.fr

† raphael.voituriez@sorbonne-universite.fr

‡ radar@technion.ac.il

- [1] A. Dussutour, V. Fourcassié, D. Helbing, and J.-L. Deneubourg, *Nature* **428**, 70 (2004).
- [2] D. E. Jackson, S. J. Martin, M. Holcombe, and F. L. Ratnieks, *Animal Behaviour* **71**, 351–359 (2006).
- [3] H. Flyvbjerg, *Nature Physics* **17**, 771–772 (2021).
- [4] J. d’Alessandro, A. Barbier-Chebbah, V. Cellerin, O. Benichou, R. M. Mège, R. Voituriez, and B. Ladoux, *Nature Communications* **12** (2021), 10.1038/s41467-021-

24249-8.

- [5] L. Tröger, F. Goirand, and K. Alim, *Proceedings of the National Academy of Sciences* **121** (2024), 10.1073/pnas.2312611121.
- [6] B. V. Hokmabad, J. Agudo-Canalejo, S. Saha, R. Golestanian, and C. C. Maass, *Proceedings of the National Academy of Sciences* **119** (2022), 10.1073/pnas.2122269119.
- [7] W. Chen, A. Izzet, R. Zakine, E. Clément, E. Vanden-Eijnden, and J. Brujic, *Physical Review Letters* **134** (2025), 10.1103/physrevlett.134.018301.
- [8] B. Toth, *The Annals of Probability* **23**, 1523 (1995).
- [9] R. Pemantle, (2007).
- [10] W. T. Kranz and R. Golestanian, *The Journal of Chemical Physics* **150** (2019), 10.1063/1.5081122.
- [11] J. Brémont, O. Bénichou, and R. Voituriez, *Physical Review Letters* **133** (2024), 10.1103/physrevlett.133.157101.
- [12] J. Brémont, L. Régnier, R. Voituriez, and O. Bénichou, *Physical Review Letters* **134** (2025), 10.1103/physrevlett.134.197103.
- [13] B. Tóth and W. Werner, “Hydrodynamic equation for a deposition model,” in *In and Out of Equilibrium* (Birkhäuser Boston, 2002) p. 227–248.
- [14] R. M. Adar and J.-F. Joanny, *Physical Review Letters* **133** (2024), 10.1103/physrevlett.133.118402.
- [15] S. Bell, J. Ackermann, A. Maitra, and R. Voituriez, *Physical Review E* **111** (2025), 10.1103/physreve.111.023405.
- [16] S. Hartman, S. D. Ryan, and B. R. Karamched, *Journal of Mathematical Biology* **89** (2024), 10.1007/s00285-024-02136-2.
- [17] A. C. Maggs, “Dynamics of a bricklayer model: multi-walker realizations of true self-avoiding motion,” (2025), arXiv:2510.00975 [cond-mat.stat-mech].
- [18] A. Gelimison, K. Zhao, C. K. Lee, W. T. Kranz, G. C. Wong, and R. Golestanian, *Physical review letters* **117**, 178102 (2016).
- [19] H. Meyer and H. Rieger, *Physical Review E* **108** (2023), 10.1103/physreve.108.034604.
- [20] H. Meyer, A. Wysocki, and H. Rieger, “Collective chemotactic search strategies,” (2024), arXiv:2409.04262 [cond-mat.soft].
- [21] Z. Mokhtari, R. I. A. Patterson, and F. Höfling, *New Journal of Physics* **24**, 013012 (2022).
- [22] E. F. Keller and L. A. Segel, *Journal of theoretical biology* **26**, 399 (1970).
- [23] E. F. Keller and L. A. Segel, *Journal of theoretical biology* **30**, 225 (1971).
- [24] E. F. Keller and L. A. Segel, *Journal of theoretical biology* **30**, 235 (1971).
- [25] M. P. Brenner, L. S. Levitov, and E. O. Budrene, *Biophysical journal* **74**, 1677 (1998).
- [26] S. Saha, R. Golestanian, and S. Ramaswamy, *Physical Review E* **89** (2014), 10.1103/physreve.89.062316.
- [27] J. Romano and A. Gambassi, “Anomalous diffusion and run-and-tumble motion of a chemotactic particle in low dimensions,” (2025), arXiv:2508.20756 [cond-mat.stat-mech].
- [28] A. Andreanov, G. Biroli, J.-P. Bouchaud, and A. Lefevre, *Physical Review E* **74**, 030101 (2006).
- [29] A. Lefevre and G. Biroli, *Journal of Statistical Mechanics: Theory and Experiment* **2007**, P07024 (2007).
- [30] S. Saha and T. Sadhu, *SciPost Physics* **17**, 033 (2024).

- [31] R. Mukherjee, S. Saha, T. Sadhu, A. Dhar, and S. Sabhapandit, *Physical Review E* **111**, 024128 (2025).
- [32] See Supplemental Material at [URL will be inserted by publisher].
- [33] D. S. Dean, *Journal of Physics A: Mathematical and General* **29**, L613 (1996).
- [34] K. Kawasaki, *Journal of statistical physics* **93**, 527 (1998).
- [35] K. A. Takeuchi, *Physica A: Statistical Mechanics and its Applications* **504**, 77–105 (2018).
- [36] M. Hairer and J. Mattingly, *Annales de l’Institut Henri Poincaré, Probabilités et Statistiques* **54** (2018), 10.1214/17-aihp840.
- [37] W. Van Saarloos, *Physics reports* **386**, 29 (2003).
- [38] J. Bernasconi and L. Pietronero, *Phys. Rev. B* **29**, 5196 (1984).
- [39] L. Dumaz and B. Tóth, *Stochastic Processes and their Applications* **123**, 1454–1471 (2013).
- [40] A. C. Maggs, *Europhysics Letters* **147**, 21001 (2024).
- [41] A. Barbier-Chebbah, O. Bénichou, and R. Voituriez, *Physical Review X* **12** (2022), 10.1103/physrevx.12.011052.
- [42] M. R. Evans, *Brazilian Journal of Physics* **30**, 42 (2000).

**Supplemental Material for: "Collective dynamics of
trail-interacting particles"**

I. DERIVATION OF STOCHASTIC DENSITY FUNCTIONAL THEORY

Our microscopic model consists of N particles distributed along L/a lattice sites, where L is the system size and a the lattice constant. The state of each site is described by two occupancy numbers, a particle occupancy ρ_i and a trail occupancy ϕ_i . For brevity, we denote the vector $\mathbf{n}_i = (\rho_i, \phi_i)$. Within a time step Δt , two types of dynamics may take place: (i) hopping between neighboring sites with probability $P_{i \rightarrow i \pm 1} = 2\rho_i k_{tr} \Delta t / (1 + \exp[H(\phi_{i \pm 1}) - H(\phi_i)])$ and (ii) deposition of a trail with probability $\rho_i k_d \Delta t$. Here, we have defined a typical translational rate k_{tr} and a typical deposition rate k_d .

We coarse-grain the microscopic lattice model into continuum equations (stochastic density functional theory) using the path-integral method of Biroli and Lefevre [1, 2] (and see also [3, 4]). We write the probability of a trajectory as

$$P \left[\{\mathbf{n}_i(t_j)\}_{i,j} \right] = \prod_{i,j} \langle \delta(\mathbf{n}_i(t_{j+1}) - \mathbf{n}_i(t_j) - \mathbf{J}_i(t_j)) \rangle_{\mathbf{J}}, \quad (1)$$

where the average is over the possible fluxes $\{\mathbf{J}_i(t_j)\}_{i,j}$. We consider the possible fluxes between site i and $i + 1$. For example, if a particle moves to the right from i to $i + 1$, we have $\mathbf{J}_i = (-1, 0) = -\mathbf{J}_{i+1}$, while a deposition at site i is given by $\mathbf{J}_i = (0, 1)$.

To construct a field theory, we introduce conjugate fluctuating variables $\hat{\mathbf{n}}_i(t_j) = (\hat{\rho}_i(t_j), \hat{\phi}_i(t_j))$, and write the Dirac delta function in Eq. (1) explicitly. This yields

$$P \left[\{\mathbf{n}_i(t_j)\}_{i,j} \right] = \mathcal{N} \int \prod_{i,j} d\hat{\mathbf{n}}_i(t_j) e^{i\hat{\mathbf{n}}_i(t_j) \cdot (\mathbf{n}_i(t_{j+1}) - \mathbf{n}_i(t_j))} \langle e^{-i\hat{\mathbf{n}}_i(t_j) \cdot \mathbf{J}_i(t_j)} \rangle_{\mathbf{J}}, \quad (2)$$

where \mathcal{N} is an irrelevant normalization prefactor. Note that i is an index when written as a subscript and is the imaginary unit otherwise.

Inserting the abovementioned probabilities and fluxes, the average is given by (the time dependence is omitted for brevity)

$$\begin{aligned} \langle e^{-i\hat{\mathbf{n}}_i \cdot \mathbf{J}_i} \rangle_{\mathbf{J}} &= 1 + k_d \rho_i dt \left(e^{-i\hat{\phi}_i} - 1 \right) \\ &+ 2k_{tr} dt \left[\frac{\rho_i}{1 + \exp[H(\phi_{i+1}) - H(\phi_i)]} \left(e^{i(\hat{\rho}_i - \hat{\rho}_{i+1})} - 1 \right) \right. \\ &\left. + \frac{\rho_{i+1}}{1 + \exp[H(\phi_i) - H(\phi_{i+1})]} \left(e^{i(-\hat{\rho}_i + \hat{\rho}_{i+1})} - 1 \right) \right]. \end{aligned} \quad (3)$$

The k_{tr} term corresponds to translation and the k_d term to deposition.

We exponentiate Eq. (3) for small dt and find that

$$P[\{\mathbf{n}_i(t_j)\}] = \int \prod_{i,j} d\hat{\mathbf{n}}_i(t_j) \exp(-S[\{\mathbf{n}_i(t_j), \hat{\mathbf{n}}_i(t_j)\}]) \quad (4)$$

with the discrete action

$$\begin{aligned} S = - \sum_{i,j} & \left[i\hat{\rho}_i(t_j)(\rho_i(t_{j+1}) - \rho_i(t_j)) + \frac{2k_{tr}\rho_i dt}{1 + \exp[H(\phi_{i+1}) - H(\phi_i)]} (e^{i(\hat{\rho}_i - \hat{\rho}_{i+1})} - 1) \right. \\ & + \frac{2k_{tr}\rho_{i+1} dt}{1 + \exp[H(\phi_i) - H(\phi_{i+1})]} (e^{i(-\hat{\rho}_i + \hat{\rho}_{i+1})} - 1) \\ & \left. + i\hat{\phi}_i(t_j)(\phi_i(t_{j+1}) - \phi_i(t_j)) + k_d \rho_i dt (e^{-i\hat{\phi}_i} - 1) \right]. \end{aligned} \quad (5)$$

The last term is the characteristic function of the Poissonian process, describing chemical deposition.

We take the limit of continuous space and time and expand to second order in the lattice spacing a . In addition, we expand the characteristic function of the Poissonian process to second order in $\hat{\phi}$. This amounts to estimating the trail distribution by a normal distribution, appropriate after sufficient deposition, due to the central limit theorem (this can also be justified by scaling arguments for large system size, where higher powers of $\hat{\phi}$ become negligible). The following action is obtained:

$$\begin{aligned} S = - \int dt dx & \left[i\hat{\rho}\dot{\rho} + i\hat{\phi}\dot{\phi} - i\hat{\phi}k_d\rho - \frac{1}{2}\rho k_d\hat{\phi}^2 \right. \\ & \left. + D(i\partial_x\rho\partial_x\hat{\rho} - \rho(\partial_x\hat{\rho})^2) + iD\rho\partial_x\hat{\rho}\partial_x H(\phi) \right], \end{aligned} \quad (6)$$

where we denote $D = k_{tr}a^2$ as the diffusion constant. In this continuum limit, the probability is given by the path integral

$$P[\mathbf{n}(t, x)] = \int \mathcal{D}\hat{\mathbf{n}} \exp(-S[\mathbf{n}(t, x), \hat{\mathbf{n}}]) \quad (7)$$

Next, we apply a Hubbard-Stratonovich transformation to the fluctuating fields,

$$\begin{aligned} P[\mathbf{n}(t, x)] &= \mathcal{N} \int \mathcal{D}\hat{\rho}\mathcal{D}\hat{\phi}\mathcal{D}\eta\mathcal{D}\xi \exp \left[\int dt dx i\hat{\rho} \left(\dot{\rho} - D\partial_x(\partial_x\rho + \rho\partial_x H(\phi)) + \partial_x(\sqrt{2D\rho}\eta) \right) \right] \\ &\times \exp \left[\int dt dx i\hat{\phi} \left(\dot{\phi} - k_d\rho - \sqrt{k_d\rho}\xi \right) \right] \times \exp \left[- \int dt dx \frac{1}{2}(\eta^2 + \xi^2) \right] \\ &= \mathcal{N} \int \mathcal{D}\eta\mathcal{D}\xi \exp \left[- \int dt dx \frac{1}{2}(\eta^2 + \xi^2) \right] \\ &\times \delta \left[\left(\dot{\rho} - D\partial_x(\partial_x\rho + \rho\partial_x H(\phi)) + \partial_x(\sqrt{2D\rho}\eta) \right) \right] \times \delta \left[\dot{\phi} - k_d\rho - \sqrt{k_d\rho}\xi \right]. \end{aligned} \quad (8)$$

This is equivalent to the equations

$$\begin{aligned}\dot{\rho} &= D\partial_{xx}\rho + D\partial_x(\rho\partial_x H(\phi)) - \partial_x(\sqrt{2D\rho}\eta), \\ \dot{\phi} &= k_d\rho + \sqrt{k_d\rho}\xi,\end{aligned}\tag{9}$$

where η and ξ are normalized, Gaussian white noises. The generalization to higher spatial dimensions is straightforward.

II. DENSITY AND TRAIL STATIC STRUCTURE FACTORS

A. Structure factors of the density

Following the analysis of the linearized dynamics in the main text, we introduce $\delta\rho = \rho - \rho_0$ and $\delta\phi = \phi - kt$. Linearizing Eqs. (9) and rescaling as in the main text, yields (in dimensionless form)

$$\begin{cases} \partial_{tt}\delta\rho + q^2\partial_t\delta\rho + khq^2\delta\rho = \frac{\Xi}{\sqrt{N}}, \\ \Xi = \sqrt{2}iq\partial_t\eta - \sqrt{k}hq^2\xi. \end{cases}\tag{10}$$

The Green's function associated with Eq. (10) is given by [Eq. (4) in the main text]

$$G(\tau, q) = \frac{e^{-q^2\tau/2}}{\sqrt{(q^2/2)^2 - q^2kh}} \sinh\left(\tau\sqrt{(q^2/2)^2 - q^2kh}\right).\tag{11}$$

In turn, the solution for the density reads

$$\delta\rho(t, q) = \frac{1}{\sqrt{N}} \int_0^t \Xi(s, q) G(t-s, q) ds.$$

The structure factor is then given by

$$\begin{aligned}S_\rho(t, q) &= \langle \delta\rho(t, q) \delta\rho(t, -q) \rangle = \frac{1}{N} \left\langle \int_0^t ds \int_0^t ds' \Xi(s, q) \Xi(s', -q) G(t-s, q) G(t-s', -q) \right\rangle \\ &= \frac{q^2}{N} \left\langle \int_0^t ds \int_0^t ds' (2\partial_s\eta(s, q)\partial_{s'}\eta(s', -q) + kh^2q^2\xi(s, q)\xi(s' - q)) G(t-s, q) G(t-s', -q) \right\rangle \\ &= \frac{q^2}{N} \left\langle \int_0^t ds \int_0^t ds' [2\eta(s, q)\eta(s', -q)G'(t-s, q)G'(t-s', -q) \right. \\ &\quad \left. + kh^2q^2\xi(s, q)\xi(s' - q)G(t-s, q)G(t-s', -q)] \right\rangle\end{aligned}$$

where we integrated by parts on s and s' . We then distribute the averages of the realization of the noises and get $\langle \eta(s, q) \eta(s', -q) \rangle = \langle \xi(s, q) \xi(s', -q) \rangle = \delta(s - s') \delta(q - q)$. The $\delta(q - q)$ is equal to unity upon rescaling with L , but should not be forgotten if one redimensionizes the equations. Finally, as $G(\tau, -q) = G(\tau, q)$,

$$S_\rho(t, q) = \frac{q^2}{N} \int_0^t ds [2G'(s, q)^2 + kh^2 q^2 G^2(s, q)]$$

For clarity, we write it explicitly

$$\begin{aligned} NS_\rho(t, q) = & \left(1 + \frac{h}{2}\right) \left\{ 1 - \frac{e^{-q^2 t}}{q^2 - 4hk} \left[-4hk + q^2 \cosh \left(qt \sqrt{q^2 - 4hk} \right) \right] \right\} \\ & + \left(1 - \frac{h}{2}\right) \frac{e^{-q^2 t}}{\sqrt{q^2 - 4hk}} q \sinh \left(qt \sqrt{q^2 - 4hk} \right) \end{aligned} \quad (12)$$

For $h > 0$, the structure factor converges at long times ($t \gg 1$) to the steady-state (SS) structure factor given in the main text:

$$S_\rho(t, q) \underset{t \rightarrow \infty}{\approx} \frac{1}{N} \left(1 + \frac{h}{2}\right) \quad (13)$$

B. Structure factor of the trail

Similar to the density, one can derive linearized equations in terms of the Fourier-transform of the trail density

$$\begin{cases} \partial_{tt} \delta \phi + q^2 (\partial_t \delta \phi + hk \delta \phi) = \frac{\Lambda}{\sqrt{N}}, \\ \Lambda = \sqrt{k} \left(\partial_t \xi + q^2 \xi - i \sqrt{2k} q \eta \right). \end{cases} \quad (14)$$

Note the different noise term $\Lambda \neq \Xi$. Making use of the Green's function defined above, we obtain

$$\delta \phi(t, q) = \int_0^t G(t - s, q) \Lambda(s, q) ds,$$

so that

$$\begin{aligned} S_\phi(t, q) = \langle \delta \phi(t, q) \delta \phi(t, -q) \rangle &= \left\langle \int_0^t ds \int_0^t ds' \Lambda(s, q) \Lambda(s', -q) G(t - s, q) G(t - s', -q) \right\rangle \\ &= \frac{k}{N} \left\langle \int_0^t ds \int_0^t ds' [(\partial_s + q^2) \eta(s, q) (\partial_{s'} + q^2) \eta(s', -q) \right. \\ &\quad \left. + 2k q^2 \xi(s, q) \xi(s', -q)] G(t - s, q) G(t - s', -q) \right\rangle \end{aligned}$$

where we have removed cross-terms in η and ξ as $\langle \eta \xi \rangle = 0$. By integrating by parts and integrating over s' , we obtain

$$S_\phi(t, q) = \frac{k}{N} \int_0^t ds [(G'(s, q) + q^2 G(s, q))^2 + 2kq^2 G^2(s, q)]$$

. Explicitly, this is given by

$$\begin{aligned} N S_\phi(t, q) = & \frac{k(2+h) + q^2}{2h q^2} \\ & + \frac{e^{-q^2 t}}{-2h q^2 (q^2 - 4hk)} \left\{ \left[4hk^2(-2-h) \right. \right. \\ & + q^2 [q^2 + k(2-3h)] \cosh \left(qt \sqrt{q^2 - 4hk} \right) \\ & \left. \left. + q \sqrt{q^2 - 4hk} [q^2 + k(2-h)] \sinh \left(qt \sqrt{q^2 - 4hk} \right) \right] \right\}. \end{aligned}$$

For $h > 0$, the steady-state structure factor reads [Eq. (5) in the main text]

$$S_\phi(t, q) \underset{t \rightarrow \infty}{\approx} \frac{k(2+h) + q^2}{2h N q^2}. \quad (15)$$

This shows that at length scales larger than $\sqrt{\frac{1}{k(2+h)}}$, the interface ϕ behaves as a Brownian motion $\delta\phi(x) = \sqrt{\frac{k(2+h)}{2h}} W(x)$ where $W(x)$ is the Wiener process. At short distances, the structure factor scales as $\sim \frac{1}{2h}$, indicating that the interface ϕ displays Poisson fluctuations of amplitude $\frac{1}{\sqrt{2h}}$.

C. Case $h = 0$

The case $h = 0$ is singular and cannot be readily obtained from the steady state defined above. Indeed, for $h = 0$, the system does not reach a steady state and the time-dependent dynamics should be properly analyzed. Inserting $h = 0$ in Eq. (9), we find that the density is decoupled from the trail field, leading to the following solution of the linear, rescaled field

$$\begin{cases} \delta\rho(t, q) = -iq\sqrt{\frac{2}{N}} \int_0^t G(t-s, q) \eta(s, q) ds, \\ G(t, q) = e^{-q^2 t}, \\ S_\rho(t, q) = \frac{1}{N} (1 - e^{-q^2 t}). \end{cases} \quad (16)$$

The trail density is solved by

$$\partial_t \delta\phi \simeq k\delta\rho + \sqrt{\frac{k}{N}} \xi,$$

solved by

$$\delta\phi(t, q) = \int_0^t \left(k\delta\rho(s, q) + \sqrt{\frac{k}{N}} \xi(s, q) \right) ds.$$

The structure factor reads

$$\begin{aligned} S_\phi(t, q) &= \langle \delta\phi(t, q) \delta\phi(t, -q) \rangle \\ &= \int_0^t ds \int_0^t ds' \left\langle \left(k\delta\rho(s, q) + \sqrt{\frac{k}{N}} \xi(s, q) \right) \left(k\delta\rho(s', -q) + \sqrt{\frac{k}{N}} \xi(s', -q) \right) \right\rangle. \end{aligned} \quad (17)$$

There are three terms to calculate

1.

$$\begin{aligned} \langle \delta\rho(s, q) \delta\rho(s', -q) \rangle &= \frac{2q^2}{N} \int_0^s du \int_0^{s'} dv G(s-u, q) G(s'-v, -q) \langle \eta_q(u) \eta_{-q}(v) \rangle \\ &= \frac{2q^2}{N} \int_0^s du \int_0^{s'} dv G(s-u, q) G(s'-v, -q) \delta(u-v) \\ &= \frac{2q^2}{N} \int_0^{\min(s, s')} G(s-u, q) G(s'-u, -q) du \end{aligned}$$

2. $\langle \xi \delta\rho \rangle = 0$

3. $\left\langle \int_0^t ds \int_0^t ds' \langle \xi(s, q) \xi(s', -q) \rangle \right\rangle = t$

Finally

$$\begin{aligned} S_\phi(t, q) &= \frac{2k^2 q^2}{N} \int_0^t ds \left\{ \int_0^s ds' \int_0^{s'} du + \int_s^t ds' \int_0^s du \right\} G(s-u, q) G(s'-u, -q) + \frac{kt}{N} \\ &= \frac{kt}{N} \left(1 + \frac{2k}{q^2} \right) + \frac{-3k^2}{q^4} + \frac{e^{-q^2 t} (-1 + 4e^{-q^2 t})}{q^4} \\ &\underset{t \gg 1}{\approx} \frac{kt}{N} \left(1 + \frac{2k}{q^2} \right) \end{aligned}$$

This means that upon rescaling by \sqrt{t} , the trail field $\delta\phi(x)/\sqrt{t}$ behaves for $q \ll \sqrt{2k}$ as a Brownian interface with effective diffusion coefficient of k^2 .

III. DYNAMIC STRUCTURE FACTORS

Upon Fourier transformation in time and space, the linearized dynamics (10) and (14) respectively read:

$$\begin{cases} [-\omega^2 + i\omega q^2 + khq^2] \delta\rho = -\frac{1}{\sqrt{N}} [\sqrt{2}q\omega\eta + \sqrt{k}hq^2\xi] \\ [-\omega^2 + i\omega q^2 + khq^2] \delta\phi = \sqrt{\frac{k}{N}} [(i\omega + q^2)\xi - i\sqrt{2k}q\eta] \end{cases}$$

We obtain

$$\begin{cases} \delta\rho(\omega, q) = \frac{i}{\sqrt{N}} \frac{\sqrt{2}q\omega\eta + \sqrt{k}hq^2\xi}{q^2\omega + i(\omega^2 - khq^2)} \\ \delta\phi(\omega, q) = \sqrt{\frac{k}{N}} \frac{\omega\xi - \sqrt{2k}q\eta - iq^2\xi}{\omega q^2 + i(\omega^2 - khq^2)} \end{cases}$$

We deduce the dynamic structure factor of the density and the trail:

$$\begin{cases} \mathcal{S}_\rho(\omega, q) = \langle |\delta\rho(\omega, q)|^2 \rangle = \frac{1}{N} \frac{q^2(kh^2q^2 + 2\omega^2)}{q^4\omega^2 + (\omega^2 - khq^2)^2} \\ \mathcal{S}_\phi(\omega, q) = \langle |\delta\phi(\omega, q)|^2 \rangle = \frac{k}{N} \frac{2kq^2 + q^4 + \omega^2}{(\omega^2 - khq^2)^2 + q^4\omega^2} \end{cases} \quad (18)$$

The $(\omega^2 - khq^2)^2$ term in the denominator is the signature of a wave mode propagating with the speed $c = \sqrt{hk}$. A comparison with numerical simulations is given in Fig 1 and confirms the contribution of this ballistic wave mode.

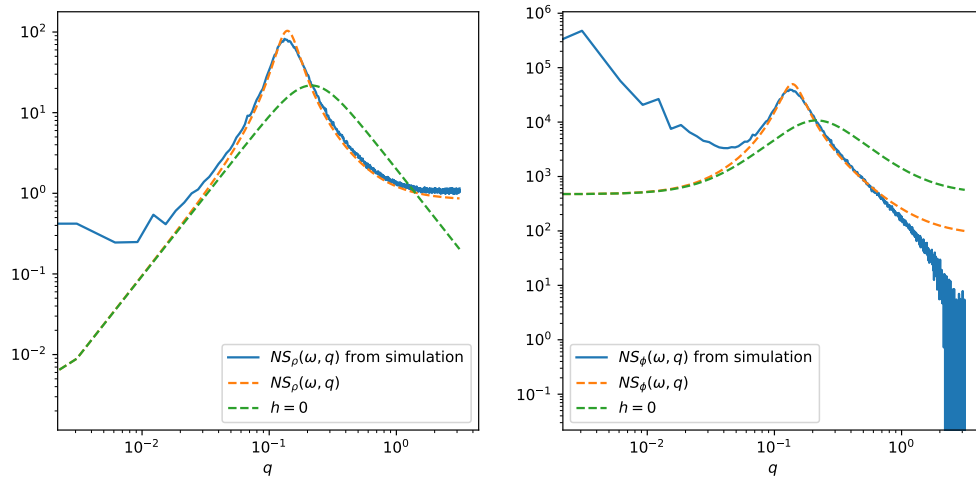


FIG. 1: Dynamical structure factor of the density (left) and of the trail (right). Solid lines are the results from simulations done with $h = 0.1, k = 1, \rho_0 = 1$ and $L = 2048$ sites, and measured at $\omega = 0.046$. Dotted lines represent theoretical predictions for $h = 0.1$ (orange) and for $h = 0$ (green).

IV. DERIVATION OF MOVING-FRONT SOLUTION IN THE REPULSIVE CASE

The mean-field equations of our theory [Eq. (1) of the main text in the absence of noise] allow for traveling-front solutions in the repulsive case ($h > 0$). While they cannot be realized in our simulations due the periodic boundary conditions, we derive them analytically. First, we assume that the fields ρ and ϕ depend on the moving coordinate $z = x - ct$, where c is the velocity. This yields the following equations

$$\begin{aligned} -c\rho' &= \rho'' + h(\rho\phi')', \\ -c\phi' &= k\rho. \end{aligned} \tag{19}$$

Combining the two equations results in the ODE

$$\rho'' = -c\rho' \left(1 - \frac{2hk}{c^2}\rho \right). \tag{20}$$

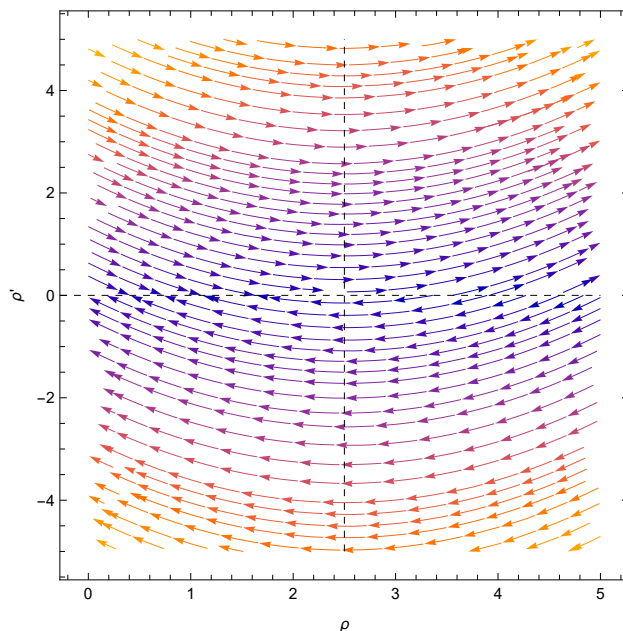


FIG. 2: Phase portrait of Eq. (20). A traveling front of decreasing density is represented by a contour that connects between ρ_l and ρ_r , for which $\rho' = 0$ (intersections with the x axis).

The phase portrait of this system is illustrated in Fig. 2. As long as $h > 0$, there is a density $\rho_* = c^2/2hk$, where ρ'' changes sign. This allows for a solution that connects $\rho_l > \rho_*$ at $z \rightarrow -\infty$ to $\rho_r < \rho_*$ at $z \rightarrow \infty$. The opposite trend (going from low to high density) does not hold. This means that it is possible to construct a steady traveling front but not a localized traveling packet within MF.

A solution to Eq. (20) can be found analytically, by inserting the ansatz

$$\rho = \rho_* \left(1 - \frac{\Delta\rho}{\rho_*} \tanh \frac{x}{\xi} \right), \quad (21)$$

with $0 < \Delta\rho/\rho_* < 1$ and ξ a coherence length. Knowing the average density $\langle\rho\rangle = \rho_0$, we require $\rho_* = \rho_0$. This provides the velocity

$$c = \sqrt{2hk\rho_0}. \quad (22)$$

Next, we calculate the derivatives and find

$$\begin{aligned} \rho' &= -\frac{\Delta\rho}{\xi} \left(1 - \tanh^2 \frac{x}{\xi} \right), \\ \rho'' &= \frac{2\Delta\rho}{\xi^2} \tanh \frac{x}{\xi} \left(1 - \tanh^2 \frac{x}{\xi} \right). \end{aligned} \quad (23)$$

Equating different powers of $\tanh x$ yields the coherence length in terms of the density difference $\xi = 2\rho_0/c\Delta\rho$. This provides a family of solutions

$$\rho = \rho_0 \left(1 - \frac{\Delta\rho}{\rho_0} \tanh \left[\frac{\Delta\rho}{2\rho_0} \sqrt{2hk\rho_0} \left(x - \sqrt{2hk\rho_0}t \right) \right] \right), \quad (24)$$

for different $\Delta\rho$.

V. MEAN FIELD SCALING SOLUTION FOR LOCALIZED INITIAL CONDITIONS

In this section, we determine the scaling solutions governing the dynamics for localized initial conditions in the vanishing-noise (mean-field) limit. We introduce the scaling ansatz

$$\begin{cases} \rho(t, x) = t^{-\alpha} f\left(\frac{x}{t^\alpha}\right), \\ \phi(t, x) = t^{-\alpha+1} F\left(\frac{x}{t^\alpha}\right), \end{cases}$$

and define the rescaled coordinate $u = x/t^\alpha$. Substituting this ansatz into Eq. (1), we obtain the coupled equations

$$\begin{cases} -\alpha t^{-\alpha-1} (fu)' = t^{-3\alpha} f''(u) + h t^{1-4\alpha} (fF')', \\ kf(u) = (1-\alpha)F(u) - \alpha u F'(u). \end{cases}$$

To capture the spatio-temporal evolution of ρ , we match the powers of t on both sides of the first equation. Two distinct regimes emerge:

- **Diffusive regime:** For $\alpha = \frac{1}{2}$,

$$\begin{cases} -\frac{1}{2}(fu)' = f'' + ht^{1/2}(fF')', \\ kf(u) = \frac{1}{2}[F(u) - uF'(u)], \end{cases}$$

where the advection term is negligible for $t \ll 1/(kh)^2$, since $F \sim kf$. In this limit, the dynamics reduces to a diffusive behavior.

- **Superdiffusive regime:** For $\alpha = \frac{2}{3}$,

$$\begin{cases} -\frac{2}{3}(fu)' = t^{-1/3}f'' + h(fF')', \\ kf(u) = \frac{1}{3}[F(u) - 2uF'(u)], \end{cases}$$

where the diffusive term becomes negligible for $t \gg 1/(kh)^3$. In this regime, the system exhibits superdiffusive scaling.

These two scaling behaviors correspond to the regimes discussed in the main text. In what follows, we focus on the superdiffusive regime with $\alpha = 2/3$. Then the first equation yields

$$f \cdot \left(\frac{2}{3}u + hF'\right) = C = 0,$$

where the last equality is due to the vanishing density at infinity. Then we have

$$\begin{cases} F(u) = \frac{1}{3h}(y_0^2 - u^2) \\ f(u) = \frac{1}{3hk}(u^2 + y_0^2/3). \end{cases}$$

In order to find y_0^2 , we know that ϕ is always positive, so u must be in $[-y_0, y_0]$ (we suppose $y_0 > 0$). Furthermore, within MF, $\int_{-y_0}^{y_0} \phi(t, x) dx = Nkt$ and $\int_{-y_0}^{y_0} \rho(t, x) dx = N$. Both conditions gives $y_0 = \left(\frac{9Nkh}{4}\right)^{1/3}$. This allows us to obtain Eq. (9) of the main text. To confirm the prediction, we made fits of the parabolas for both fields. We set the notation for the parabola fitting function to be $P(x) = ax^2 + b$. We sum up the results in Fig. 3.

VI. ATTRACTIVE CASE: SCALING OF q_* WITH k

We plot in Fig. 4 the scaling of q_* with k in the strong interacting regime $|h| \gg 1$, as mentioned in the main text.

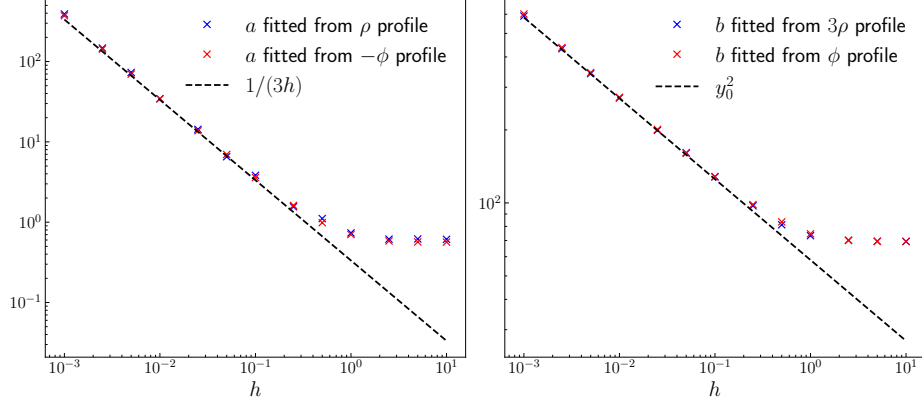


FIG. 3: Comparison of the theoretical predictions with the fitted parabola $P(x) = ax^2 + b$ parameters a (left) and b (right). Simulations are performed with $N = 1024$ and $k = 1$ and averaged over 100 realizations.

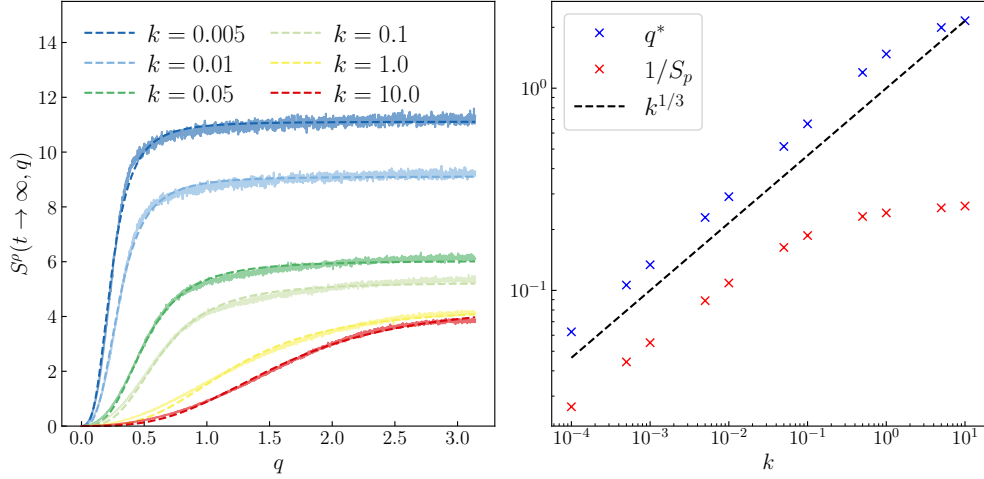


FIG. 4: The asymptotic value of the structure factor S_p (left) and characteristic wavevector q_* (right) as a function of k for $h = -10$. The theoretical scaling is plotted in dashed black. Simulations are made for parameters values $L = 4096$, $k_{tr} = 1$, and averaged 10^4 times.

VII. NUMERICAL SIMULATIONS

All numerical simulations were performed using the Gillespie algorithm implemented in Julia. All scripts required to reproduce the figures and analyses are available in a public repository:

github.com/PaulPineauGit/Collective-dynamics-of-trail-interacting-particles.

VIII. SUPPLEMENTARY MOVIES

Videos of the dynamics are available at the GitHub repertory quoted above and [here](#). There are done for the following values of parameters:

- $L = 256, h = -0.01, k_{tr} = 1, k = 1, \rho_0 = 1$
- $L = 256, h = -0.1, k_{tr} = 1, k = 1, \rho_0 = 1$
- $L = 256, h = 0.1, k_{tr} = 1, k = 1, \rho_0 = 1$

-
- [1] A. Andreanov, G. Biroli, J.-P. Bouchaud, and A. Lefevre, Physical Review E **74**, 030101 (2006).
 - [2] A. Lefevre and G. Biroli, Journal of Statistical Mechanics: Theory and Experiment **2007**, P07024 (2007).
 - [3] S. Saha and T. Sadhu, SciPost Physics **17**, 033 (2024).
 - [4] R. Mukherjee, S. Saha, T. Sadhu, A. Dhar, and S. Sabhapandit, Physical Review E **111**, 024128 (2025).